Phosphorylation of serine 367 of FOXC2 by p38 regulates ZEB1 and breast cancer metastasis, without impacting primary tumor growth

SJ Werden[1]*, N Sphyris[1]*, TR Sarkar[1], AN Paranjape[1], AM LaBaff[4], JH Taube[1,$], BG Hollier[1]‡, EQ Ramirez-Peña[1], R Soundararajan[1], P den Hollander[1], E Powell[5], GV Echeverria[5], N Miura[6], JT Chang[7], H Piwnica-Worms[5], JM Rosen[8,9] and SA Mani[1,2,3,§]

[1]Department of Translational Molecular Pathology, The University of Texas MD Anderson Cancer Center, Houston, Texas 77030, USA.

[2]Metastasis Research Center, The University of Texas MD Anderson Cancer Center, Houston, Texas 77030, USA.

[3]Center for Stem Cell and Developmental Biology, The University of Texas MD Anderson Cancer Center, Houston, Texas 77030, USA.[4]Molecular and Cellular Oncology, The University of Texas MD Anderson Cancer Center, Houston, Texas 77030, USA.

[5]Department of Cancer Biology, The University of Texas MD Anderson Cancer Center, Houston, Texas 77030, USA.

[6]Department of Biochemistry, Hamamatsu University School of Medicine, Hamamatsu, Japan.

[7]Department of Integrative Biology and Pharmacology, University of Texas Health Science Center at Houston, Houston, Texas, USA

[8]Program in Developmental Biology, Baylor College of Medicine, Houston, TX 77030, USA.

[9]Department of Molecular and Cellular Biology, Baylor College of Medicine, Houston, TX 77030, USA.

‡Present address: Australian Prostate Cancer Research Centre-Queensland, Queensland University of Technology, Brisbane, 4102, Australia

$Present address: Baylor University, Waco, Texas 76798

*SJW and NS share co-first authorship of this article.

[§]**Correspondence:** Dr. SA Mani, Department of Translational Molecular Pathology, The University of Texas MD Anderson Cancer Center, 2130 W. Holcombe Blvd, Houston, TX 77030. Phone: 713-792-9638. Fax: 713-834-6083. E-mail: smani@mdanderson.org

Running Title: Targeting p38-FOXC2 crosstalk inhibits metastasis

Financial Support: This research was supported by grants from the National Institute of Health (5RO1CA155243) and the Cancer Prevention and Research Institute of Texas (**RP-130485)**. SAM is an American Cancer Society M. Patricia Alexander Research Scholar (121958-RSG-12-102-01-DDC). SJW received a Susan G. Komen Breast Cancer Foundation Postdoctoral Fellowship. Flow cytometry, animal imaging and histophathology were in part funded by the Cancer Center Support Grant from the National Cancer Institute (5P30CA016672).

Supplementary Figure Legends

Supplementary Figure 1. SB203580 treatment decreases FOXC2 immunostaining but neither SB203580 nor p38 shRNA impact *FOXC2* transcript levels. (**a**) The indicated cells were immunostained with antibodies against p-p38 (green) and FOXC2 (red). Nuclei were counterstained with DAPI (blue). Scale bar, 20 μm. (**b**) The indicated cells were treated with vehicle or SB203580 and subsequently immunostained with antibodies against FOXC2 (green). Nuclei were counterstained with DAPI (blue). Scale bar, 20 μm. (**c**) The relative expression of *FOXC2* mRNA in the indicated cells, treated with vehicle or SB203580, was determined by qRT-PCR. *GAPDH* was used as the reference gene. (**d**) The relative expression of *FOXC2* mRNA in the indicated cells, transduced with control shRNA (shControl) or *p38* shRNA (shp38), was determined by qRT-PCR. *GAPDH* was used as the reference gene.

Supplementary Figure 2. Monitoring mammary tumor progression and the effect of SB203580 treatment. (**a**) RFP/luciferase-labeled 4T1 cells were orthotopically injected into mice, subsequently treated daily with vehicle (left panels) or SB203580 (right panels). Bioluminescent imaging was used to monitor weekly primary tumor growth. (**b**) The bioluminescent signal from the primary tumors from mice in (a) was quantified and plotted as the total photon flux emitted by the primary mammary tumors over time. (**c**) Macroscopic images of the lungs from mice in (a), harvested at 3, 4, 5 and 6 weeks, after implantation and treatment. n=5 mice per group. Veh=vehicle; SB=SB203580. (**d**) Representative hematoxylin and eosin staining of lung sections, harvested from mice described in (a), at 5 weeks after implantation and treatment. Scale bar, 100 μm.

Supplementary Figure 3. p38 inhibition compromises colonization in an experimental metastasis model. (**a**) Luciferase-labeled MDA-MB-231 cells were injected into NOD/SCID mice via the tail-vein. Starting 48 h post-implantation, the mice were treated daily with vehicle or SB203580 (n=6 mice per group). The emergence of lung metastases was monitored by bioluminescent imaging. Representative bioluminescent images, at 8 weeks post-implantation, are shown. (**b**) The Kaplan-Meier event-free survival curves of mice, injected with luciferase-labeled MDA-MB-231 cells via the tail-vein, and subsequently treated daily with vehicle or SB203580, were generated. n=6 mice per group. The Gehan-Breslow-Wilcoxon method was used to compare the Kaplan-Meier survival curves and compute the corresponding p values. (**c**) Luciferase-labeled MDA-MB-231 cells, transduced with either control shRNA (shControl) or *p38* shRNA (shp38), were injected into NOD/SCID mice via the tail-vein (n=7 mice per group). The emergence of lung metastases was monitored by bioluminescent imaging. Representative bioluminescent images, at 9 weeks post-implantation, are shown. (**d**) The Kaplan-Meier event-free survival curves of mice injected via the tail-vein with luciferase-labeled MDA-MB-231 cells, transduced with *p38* shRNA (shp38) or control shRNA (shControl), were generated. n=7 mice per group. The Gehan-Breslow-Wilcoxon method was used to compare the Kaplan-Meier survival curves and compute the corresponding p values.

Supplementary Figure 4. p38 inhibition compromises EMT and the formation of invadopodia. (**a**) SB203580 and SB202190 affect EMT markers, but not Akt activity. HLME-Snail cells were treated with 20μM of SB203580, SB202190, or vehicle for 24hrs. Cells were lysed and the corresponding lysates were analyzed by immunoblotting for p-

Akt, Akt, FOXC2 and ZEB1. β-actin was used as a loading control. (**b**) HMLE-Snail cells were plated on FITC-conjugated gelatin (green) and treated with vehicle or SB203580. After 16 h, the cells were fixed and stained with fluorescent phalloidin, which binds to F-actin, and the nuclei were counterstained with DAPI to facilitate visualization of the cells. Areas of gelatin degradation, appearing as punctate black areas beneath the cells, are indicated by white arrows. Representative images are shown. Scale bar, 20 μm.

Supplementary Figure 5. p38 interacts with FOXC2. (**a**, **b**) HEK293T cells were transfected with Myc-FOXC2 and HA-p38 or a kinase-dead mutant of p38 (HA-p38-DN) and subjected to immunoprecipitation (IP) with anti-HA (p38), anti-Myc (FOXC2) or control IgG followed by immunoblotting (IB) with antibodies as indicated.

Supplementary Figure 6. ZEB1 knockdown affects the mammosphere-forming ability. (a) SUM159 control cells (FF3) and shZEB1 cells were subjected to a sphere-formation assay. Data are presented as the mean number of spheres formed/500 seeded cells ± SEM. (b) SUM159 FF3 and shZEB1 cells were lysed and the corresponding lysates were analyzed by immunoblotting for p-ATF2, ATF2, FOXC2 and ZEB1. β-actin was used as a loading control.

Supplementary Figure 1

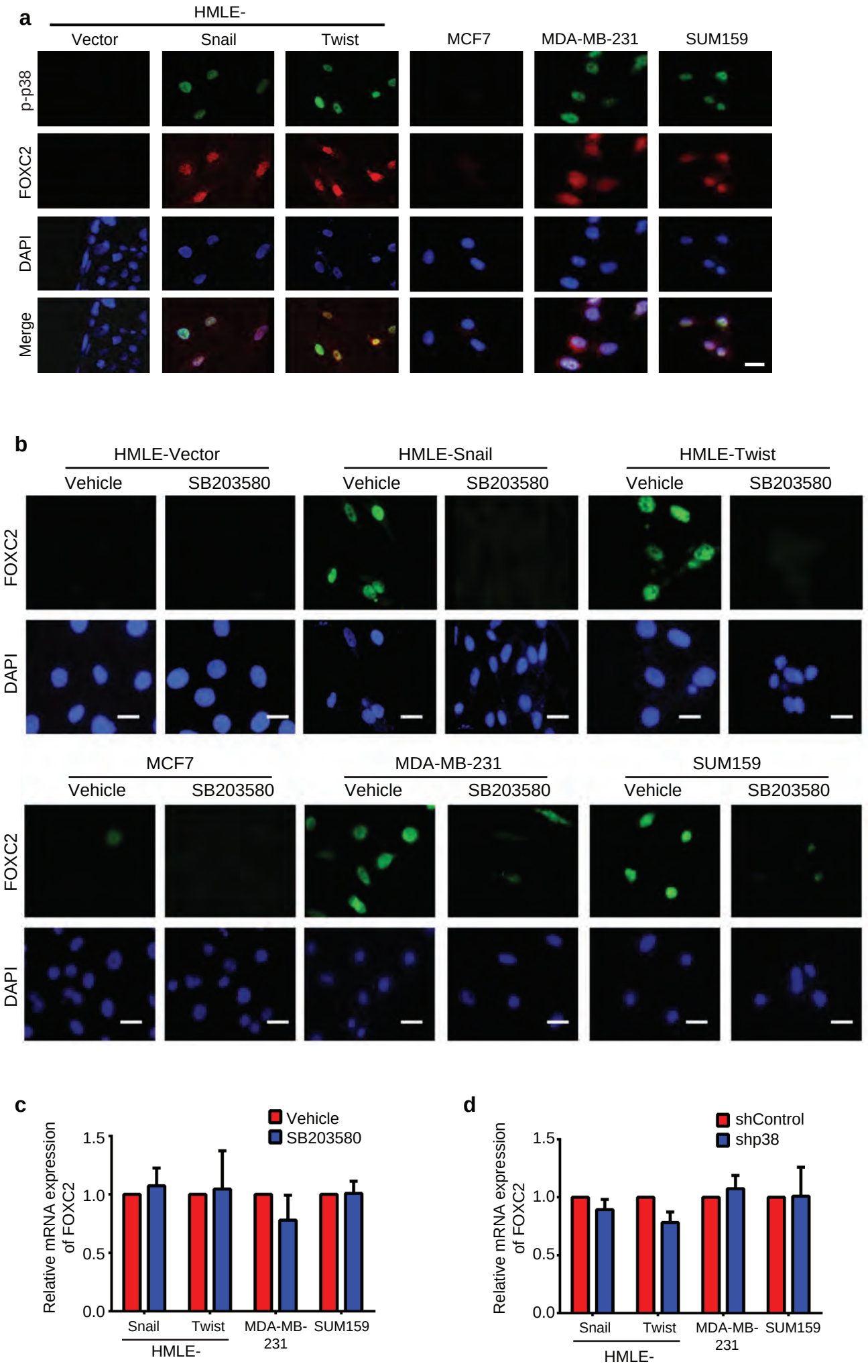

Supplementary Figure 2

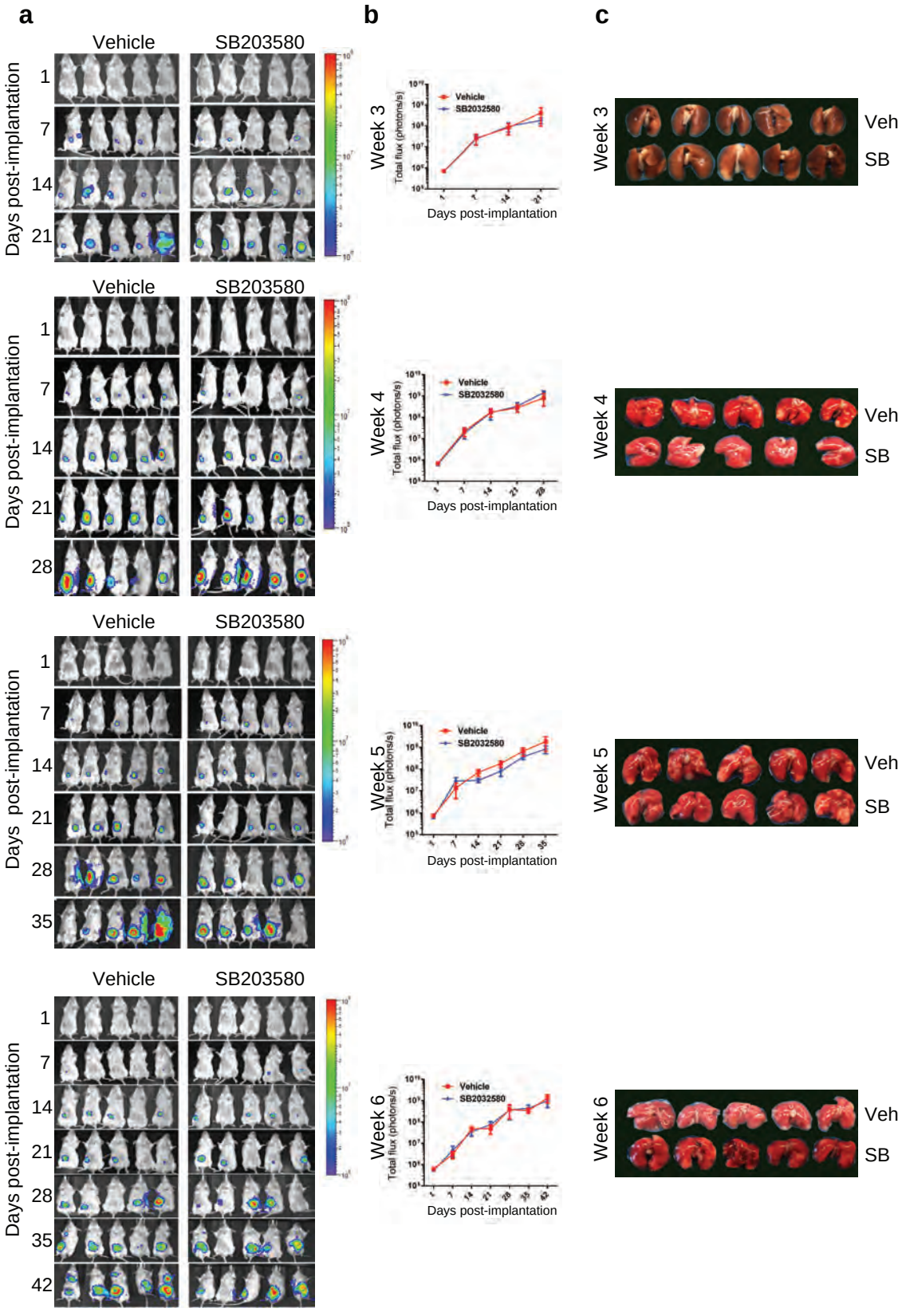

Supplementary Figure 3

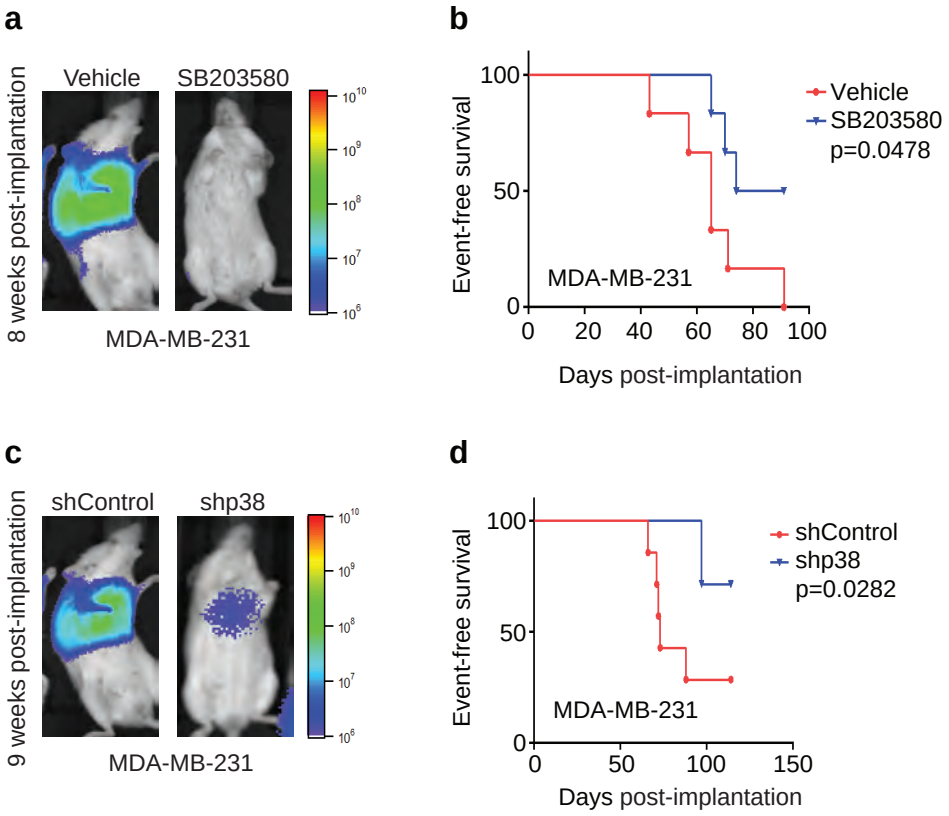

Supplementary Figure 4

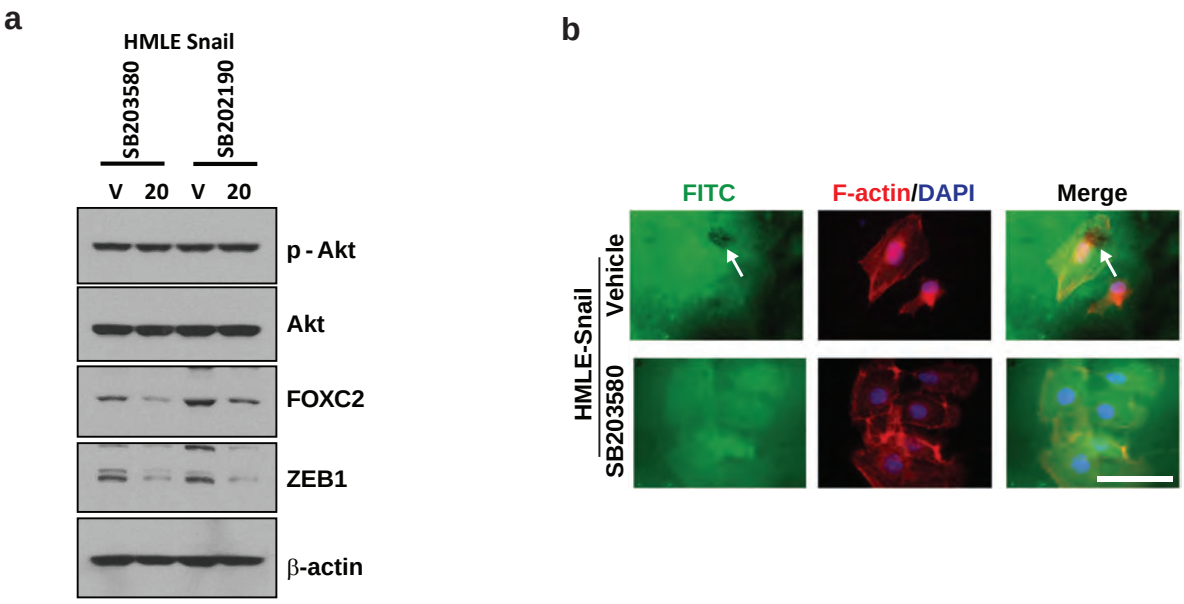

Supplementary Figure 5

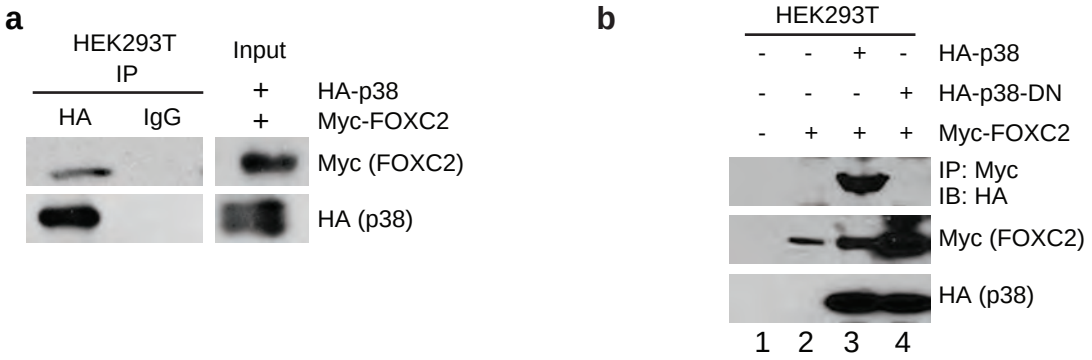

Supplementary Figure 6